IL NUOVO CIMENTO **47 C** (2024) 46
DOI 10.1393/ncc/i2024-24046-7

COLLOQUIA: COMEX7

A new approach to nuclear level densities: The QRPA plus boson expansion

S. GORIELY(1), S. HILAIRE(2), S. PÉRU(2) and G. GOSSELIN(2)

(1) *Institut d'Astronomie et d'Astrophysique, Université Libre de Bruxelles - Campus de la Plaine CP 226, 1050 Brussels, Belgium*
(2) *CEA, DAM, DIF - F-91297 Arpajon, France*

received 31 October 2023

Summary. — Nuclear level densities play a key role in many nuclear applications. To go beyond the usual particle-independent approximation, a conceptually new approach based on the boson expansion of QRPA excitations is described. The calculated nuclear level densities are shown to follow an energy dependence close to a constant-temperature formula at energies above a few MeV, but present a rather narrow spin distribution. A quite remarkable agreement is obtained with experimental s-wave resonance spacings and Oslo data, at least for the 48 even-even nuclei considered in the present study.

1. – Introduction

Nuclear level densities (NLDs) play a key role in the modelling of nuclear reactions, hence in the evaluation of the nuclear data and in many nuclear applications. It has been a field of research for years going back at least to 1936 with Bethe's pioneering work [1]. Based on the corresponding Fermi Gas model, a large number of analytical formulas have been proposed to describe not only the exponential increase of levels with excitation energies, but also the impact of shell, pairing and collective effects (see, *e.g.*, ref. [2] and references therein). Such models mainly resort to phenomenological parameters adjusted to scarce experimental data or deduced from systematics. Their predictions are expected to be reliable for nuclei not too far from experimentally accessible regions and at energies where experimental constraints exist, but are questionable, in particular, when dealing with exotic nuclei. To face such difficulties, it is preferable to rely on as fundamental (microscopic) as possible methods based on physically sound models.

Microscopic models of NLD have been developed (see, *e.g.*, [3-9] and references therein), but they are seldom used for practical applications due to (*i*) their lack of accuracy in reproducing experimental data (especially when considered globally on a large

data set), (*ii*) their restricted flexibility in comparison with highly parametrized analytical expressions, or (*iii*) their limitation when applied to the large set of nuclei needed for applications. The combinatorial approach followed in refs. [3,4] clearly demonstrated that such models can compete with the statistical ones in the global reproduction of experimental data. This approach provides energy, spin and parity dependence of NLD, and, at low energies, describes the non-statistical limit which, by definition cannot be described by the traditional statistical formulas. Such a non-statistical behaviour can have a significant impact on cross section predictions, particularly when calculating cross sections known to be sensitive to spin or parity distributions such as for isomeric production or low-energy neutron capture [10]. However, the combinatorial method also offers room for improvement because of the phenomenological aspects of some ingredients it contains as well as the fundamental assumption of independent particles it entails, as all statistical approach also do: both aspects could hamper its microscopic nature, and consequently its predictive power, especially at the lowest energies.

When considering publicly available global NLD models providing predictions for a large number of nuclei, only a limited number of methods are available. These include one of the many analytical forms of the Fermi Gas model (see, *e.g.*, [2, 11]), the statistical model based on mean-field single-particle scheme and pairing properties [12] and the combinatorial approach [3,4]. Such a collection of NLD models is in particular available in the TALYS reaction code [13]. All these models more or less reproduce equally well the overall set of NLD experimental data that essentially consist of low-lying levels, s-wave resonance spacings at the neutron separation energy [2] and the Oslo data [14,15]. They are all based on the independent-particle approximation, so that at energies below a few MeV, they all fail to reproduce the detailed structure-dependent distribution of low-lying levels, in particular the vibrational ones. More microscopic approaches, like the shell model and its many variants, include correlations beyond mean-field theory but their applications, even within the shell model Monte Carlo method [7,8], are restricted to medium-mass nuclei and can hardly be extended to the thousands of nuclei of interest in nuclear applications.

For this reason, a conceptually new approach beyond the independent-particle approximation and still tractable at large scale has been proposed [16]. This so-called QRPA+BE method is based on the boson expansion of quasi-particle random phase approximation (QRPA) excitations. After describing the methodology, the energy, parity and spin distributions of the newly estimated NLDs are compared with other global models and available experimental data.

2. – The QRPA+BE method

Considering the underlying quasi-boson approximation, all QRPA states are boson excitations acting on the QRPA vacuum. The latter can be built from the HFB ground state with an exponential form of boson operators [17]. Such a QRPA formalism based on axially-symmetric-deformed HFB equations solved in a finite harmonic oscillator basis in cylindrical coordinates has been described in details in refs. [18-23]. This QRPA method using the D1M Gogny force [24] has proven its capacity to predict the E1 and M1 photon strength functions [21,25] as well as the Gamow-Teller response [23,26] with a high degree of reliability. The QRPA method has also shown its capacity to reproduce rather well low-lying vibrational levels [20,25]. In the present study, the D1M+QRPA approach is used to estimate all intrinsic states with angular momentum projection up to $K_{\max} = 9$. For nuclei up to $Z = 74$, QRPA calculations are performed without

any energy cutoff on the two-quasi-particle states energies. In contrast, to decrease the computational time, for $Z \geq 76$ nuclei, a cutoff energy $\varepsilon_c = 120$ MeV is applied for practical consideration. Since for heavy systems like actinides, it remains computerwise extremely heavy to consider large basis dimension and large cutoff energies of the two-quasi-particle states, nuclei with $Z > 82$ are not considered at this stage. Despite such a large cutoff, spurious states are known to appear for specific K^π blocks and need to be omitted, as described in ref. [16].

To go beyond the QRPA excitations, the intrinsic level density, including vibrational states, can be derived using a generalised boson partition function, as detailed in refs. [16, 27]. The present approach is conceptually different from the previous works the combinatorial approach [3, 27, 28], since there is no need to perform here any convolution with incoherent particle-hole excitations, those being implicitly included in the QRPA phonons.

QRPA excitation energies with D1M or D1S interactions tend to be overestimated (see fig. 1 of ref. [25]) by typically 100-200 keV. For this reason, all QRPA K^π energies are lowered by 150 keV before applying the boson expansion. Similarly, the D1M interaction is known to give rather strong shell effects due to its low effective mass leading to a systematic overestimate of QRPA excitations for closed shell nuclei. In particular, we find the first ^{208}Pb 2^+ and 3^- levels to be overestimated by typically 0.6 MeV. For this reason, a constant energy shift of -0.65 MeV is applied to all K^π components for nuclei with Z, N or $N+2$ corresponding to magic numbers.

Finally, the QRPA+BE NLD is obtained for spherical nuclei from the state density in the laboratory frame $\omega_{\rm tot}(U, M = J, \pi)$ through

$$\rho_{\rm s}(U, J, \pi) = \omega_{\rm tot}(U, M = J, \pi) - \omega_{\rm tot}(U, M = J + 1, \pi) \ . \tag{1}$$

For deformed nuclei, the NLD is derived by including rotational bands on top of each band head through the usual expression [28]

$$\begin{aligned} \rho_{\rm d}(U, J, \pi) = \ & \frac{1}{2} \Big[\sum_{K=-J, K\neq 0}^{J} \omega_{\rm tot}(U - E_{rot}^{J,K}, K, \pi) \Big] \\ & + \omega_{\rm tot}(U - E_{rot}^{J,0}, 0, \pi) \Big[\delta_{(J\ even)}\, \delta_{(\pi=+)} + \delta_{(J\ odd)}\, \delta_{(\pi=-)} \Big]. \end{aligned} \tag{2}$$

where, the symbol $\delta_{(x)}$ (defined by $\delta_{(x)} = 1$ if x holds true and 0 otherwise) restricts the rotational bands built on intrinsic states with spin projection $K = 0$ and parity π to the levels sequences $0, 2, 4, ...$ for $\pi = +$ and $1, 3, 5, ...$ for $\pi = -$. The rotational energy is obtained with the well-known expression [29],

$$E_{rot}^{J,K} = \frac{J(J+1) - K^2}{2\mathcal{J}_\perp}, \tag{3}$$

where $\mathcal{J}_\perp$ is the Belyaev moment of inertia of a nucleus rotating around an axis perpendicular to the symmetry axis, as determined within the HFB approach with D1M effective interaction. The Belyaev moment of inertia is typically about 30% lower than the experimental one and is consequently systematically increased by 30% in the present calculations.

Finally, it is well known that there is a sharp transition appearing when selecting either eq. (1) or (2) (*i.e.*, if a nucleus is spherical or deformed). Both spherical and well-deformed nuclei can be properly described in the present framework. However, it fails to describe intermediate cases for which an exact projection technique should be included. For this reason, to smooth out the difficult cases of transitional deformation, a phenomenological damping function $\mathcal{F}$ is introduced [3, 28] such that

$$\rho(U,J,\pi) = \Big[1-\mathcal{F}\Big]\rho_s(U,J,\pi) + \mathcal{F}\rho_d(U,J,\pi). \tag{4}$$

We consider, as in ref. [4], an expression depending on the quadrupole deformation parameter β_2 only which reads

$$\mathcal{F} = 1 - \Big[1+\mathrm{e}^{(\beta_2-0.18)/0.04}\Big]^{-1}, \tag{5}$$

where the parameters have been adjusted in order to reproduce at best the measured s-wave mean spacings.

3. – The QRPA+BE level densities

The energy dependence of the QRPA+BE total NLD is compared in fig. 1 for the deformed ^{170}Yb nucleus with 5 alternative and widely used NLD models. Above a few MeV, the QRPA+BE NLD is seen to follow an energy dependence rather similar to the constant-temperature formula. Deviations from a simple exponential law are however found at low energies and depict the complex nuclear structure properties. As shown in ref. [16], the equiparity is achieved at an excitation energy in the QRPA+BE case higher than in the particle-independent combinatorial approach. The spin distribution of the QRPA+BE NLD is also illustrated in fig. 1 for ^{170}Yb and compared with predictions by the same alternative models. Significantly narrower spin distributions are obtained with the QRPA+BE NLDs with a spin cutoff factor close to 3-4 at energies around the separation energy. Such a low spin cutoff parameter ($\sigma = 2.9 \pm 0.2$) was extracted for example by (p,p$'$) experiment on ^{150}Nd isotope at this energy [30]. Although the narrow spin distribution experimentally deduced though the side-feeding method was interpreted as resulting from the specific reaction mechanism inefficiently populating all spins at such an energy, the QRPA+BE prediction suggests that such a narrow spin distribution may actually correspond to the intrinsic one expected at this energy.

The QRPA+BE s-wave spacings for 48 even-even nuclei are compared in fig. 3 with experimental data [2]. An overall excellent agreement by a factor $f_{\rm rms} = 1.65$ is obtained, showing the relevance of the newly proposed QRPA+BE approach to reproduce experimental data in the wide range of $74 \leq A \leq 209$ globally within a factor of 2 and of no more than a factor of 3.8. This level of accuracy is similar to (or even better than) the one found by the most successful global NLD models [2]. In particular, on the same set of D_0 values, $f_{rms} = 1.5$ and 2.4 for the Cst-T and HFB+comb models, respectively. Note that the energy shift applied to the QRPA energies by -0.15 MeV typically reduces the NLD by a factor of 2 and the -0.65 MeV shift for closed-shell nuclei by a factor between 5 and 25, as shown in fig. 3. This simulation also shows how important it is to accurately estimate in particular the lowest QRPA energies. For this reason, this approach to NLD also represents a stringent test of the interaction used in the QRPA calculation. In

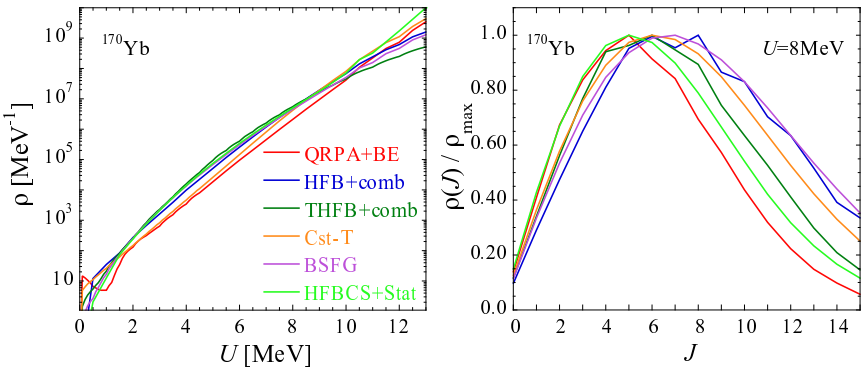

Fig. 1. – (Color online) Comparison, for ^{170}Yb, between QRPA+BE total NLDs (left panel) and normalised spin distribution at 8 MeV (right panel) and 5 widely used model predictions, namely the HFB plus combinatorial (HFB+comb) [3], the temperature-HFB plus combinatorial (THFB+comb) [4], the constant temperature (Cst-T) [11], the Back-Shifted Fermi Gas (BSFG) [11] and the HFBCS plus statistical model (HFBCS+Stat) [12] models.

particular an overestimation of the QRPA energies, for both D1S or D1M interactions, leads to an underestimate of the NLD after the boson expansion.

The energy distribution of the QRPA+BE NLD is finally compared with Oslo measurements in fig. 4 for ^{172}Yb using the same procedure as in ref. [15], *i.e.*, the theoretical NLD formula is adjusted through a scaling factor and an energy shift to reproduce at

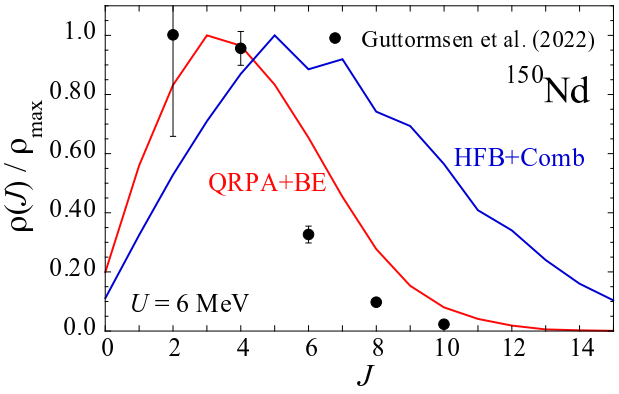

Fig. 2. – (Color online) Comparison between QRPA+BE and HFB+comb normalised spin distribution of ^{150}Nd at $U = 6$ MeV as a function of the spin J (in $\hbar$). Also included is the spin distribution extracted by the side-feeding method [30] leading to an estimated spin cutoff parameter $\sigma = 2.9 \pm 0.2$.

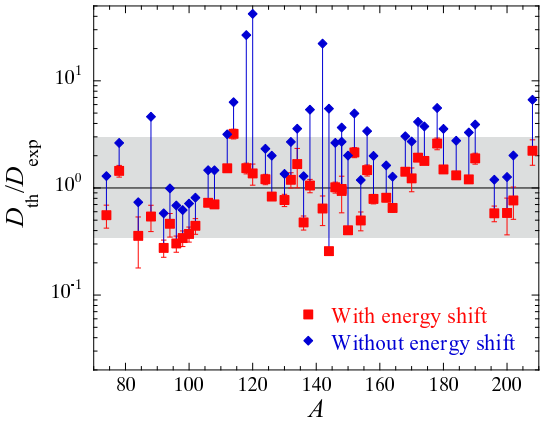

Fig. 3. – (Color online) Ratio of QRPA+BE (D_{th}) to the experimental (D_{exp}) [2] s-wave neutron resonance spacings for 48 even-even compound nuclei. The blue diamonds are obtained without including any energy shift to the QRPA excitation energies. The red squares correspond to the final results when including a -0.15 MeV shift to all excitation energies except to the semi-magic nuclei for which a shift of -0.65 MeV is applied. The red error bars correspond to the experimental uncertainties.

best the experimental s-wave spacing and the Oslo data are normalised to the theoretical NLD at the highest measured energies. Both QRPA+BE and HFB+comb NLDs are seen to be in good agreement with data, but only QRPA+BE predictions agree at the lowest energies. The impact of these NLD models on the ^{171}Yb(n,γ)^{172}Yb cross sections is shown in fig. 4 where a better agreement is found with the QRPA+BE NLDs. More comparisons between QRPA+BE and Oslo NLDs can be found in ref. [15].

4. – Conclusions

To go beyond the usual particle-independent approximation, a new approach based on the boson expansion of QRPA excitations has been proposed [16]. The calculated NLDs are shown to follow an energy dependence close to a constant-temperature formula at energies above a few MeV, but present a spin distribution that is rather narrower than what is predicted by other models. The NLDs are also found to achieve equiparity at energies higher than what is obtained within the combinatorial approach. For the 48 even-even nuclei below Pb for which experimental s-wave spacings are available, a quite remarkable agreement with s-wave resonance spacings is found, provided the QRPA excitation are globally shifted down. Excellent agreement with Oslo data is also found, highlighting the relevance of the present approach.

The QRPA+BE approach is restricted at the present time to even-even systems but will be in the future extended to nuclei with an odd number of nucleons. Since these systems breaks the time-reversal symmetry but also the boson nature of the QRPA excitations, they should be treated with special care. Similarly, a special attention will be given to nuclei heavier than Pb for which some truncations may need to be imposed to the QRPA calculation to remain tractable. While a long-term goal will be to improve

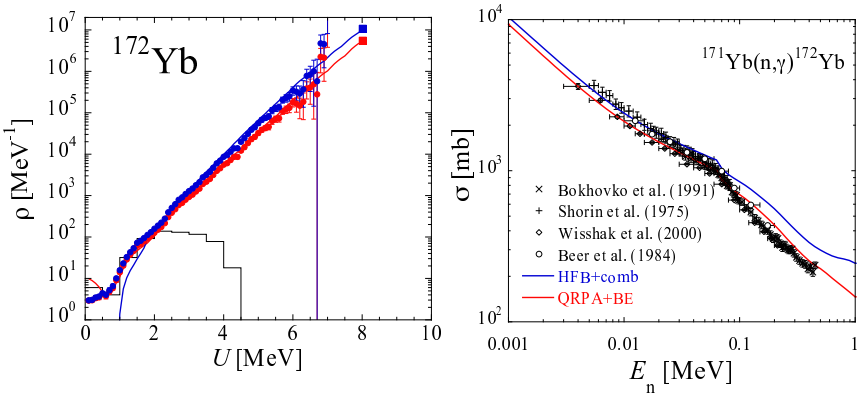

Fig. 4. – (Color online) Left panel: Theoretical and renormalised Oslo NLDs for ^{172}Yb. The solid line represents the NLD extracted from known discrete levels on an energy bin $\Delta E = 0.5$ MeV. The solid circles correspond to the Oslo data [14] and the solid lines to the present QRPA+BE NLD predictions. The full square at $U = S_n$ corresponds to the total level density extracted for the QRPA+BE NLD model after renormalisation on the experimental D_0 value. Right panel: Comparison between experimental and theoretical ^{171}Yb(n,γ)^{172}Yb cross sections when using either the QRPA+BE or HFB+comb NLDs shown in the right panel. Experimental cross sections [31-34] are given by black symbols.

the interaction to accurately describe the QRPA excitations, some refined systematics regarding their energy renormalisation can provide in the mean time a phenomenological approach that can further increase the accuracy of NLD predictions. A large-scale calculation of QRPA+BE NLD for applications is foreseen in the future.

* * *

SG acknowledges financial support from F.R.S.-FNRS (Belgium). This work was supported by the Fonds de la Recherche Scientifique - FNRS and the Fonds Wetenschappelijk Onderzoek - Vlaanderen (FWO) under the EOS Project No O000422 and O022818F.

REFERENCES

[1] Bethe H., *Phys. Rev.*, **50** (1936) 332.
[2] Capote R., Herman M., Oblozinsky P., Young P., Goriely S., Belgya T., Ignatyuk A., Koning A., Hilaire S., Plujko V., Avrigeanu M., Bersillon O., Chadwick M., Fukahori T., Ge Z., Han Y., Kailas S., Kopecky J., Maslov V., Reffo G., Sin M., Soukhovitskii E. and Talou P., *Nucl. Data Sheets*, **110** (2009) 3107.
[3] Goriely S., Hilaire S. and Koning A. J., *Phys. Rev. C*, **78** (2008) 064307.
[4] Hilaire S., Girod M., Goriely S. and Koning A. J., *Phys. Rev. C*, **86** (2012) 064317.
[5] Uhrenholt H., Aberg S., Dobrowolski A., Døssing T., Ichikawa T. and Möller P., *Nucl. Phys. A*, **913** (2013) 127.
[6] Døssing T. and Aberg S., *Eur. Phys. J. A*, **55** (2019) 249.
[7] Alhassid Y., Bonett-Matiz M., Liu S. and Nakada H., *Phys. Rev. C*, **92** (2015) 024307.

[8] Alhassid Y., *Eur. Phys. J. A*, **51** (2015) 171.
[9] Zelevinsky V. and Karampagia S., *EPJ Web of Conferences*, **194** (2018) 01001.
[10] Goko S., Utsunomiya H., Goriely S., Makinaga A., Kaihori T., Hohara S., Akimune H., Yamagata T., Lui Y.-W., Toyokawa H., Koning A. J. and Hilaire S., *Phys. Rev. Lett.*, **96** (2006) 192501.
[11] Koning A. J., Hilaire S. and Goriely S., *Nucl. Phys. A*, **810** (2008) 13.
[12] Demetriou P. and Goriely S., *Nucl. Phys. A*, **695** (2001) 95.
[13] Koning A., Hilaire S. and Goriely S., *Eur. Phys. J. A*, **59** (2023) 131.
[14] Oslo database, *Level densities and gamma-ray strength functions* (2021) `http://www.mn.uio.no/fysikk/english/research/about/infrastructure/OCL/nuclear-physics-research/compilation/`.
[15] Goriely S., Larsen A. C. and Mücher D., *Phys. Rev. C*, **106** (2022) 044315.
[16] Hilaire S., Goriely S., Péru S. and Gosselin G., *Phys. Lett. B*, **843** (2023) 137989.
[17] Ring P. and Schuck P., *The Nuclear Many-Body Problem* (Springer) 2004.
[18] Péru S. and Goutte H., *Phys. Rev. C*, **77** (2008) 044313.
[19] Péru S., Gosselin G., Martini M., Dupuis M., Hilaire S. and Devaux J.-C., *Phys. Rev. C*, **83** (2011) 014314.
[20] Péru S. and Martini M., *Eur. Phys. J. A*, **50** (2014) 88.
[21] Martini M., Péru S., Hilaire S., Goriely S. and Lechaftois F., *Phys. Rev. C*, **94** (2016) 014304.
[22] Goriely S., Hilaire S., Péru S., Martini M., Deloncle I. and Lechaftois F., *Phys. Rev. C*, **94** (2016) 044306.
[23] Deloncle I., Péru S. and Martini M., *Eur. Phys. J. A*, **53** (2017) 170.
[24] Goriely S., Hilaire S., Girod M. and Péru S., *Phys. Rev. Lett.*, **102** (2009) 242501.
[25] Goriely S., Hilaire S., Péru S. and Sieja K., *Phys. Rev. C*, **98** (2018) 014327.
[26] Martini M., Péru S. and Goriely S., *Phys. Rev. C*, **89** (2014) 044306.
[27] Hilaire S., Delaroche J.-P. and Girod M., *Eur. Phys. J. A*, **12** (2001) 169.
[28] Hilaire S. and Goriely S., *Nucl. Phys. A*, **779** (2006) 63.
[29] Døssing T. and Jensen A., *Nucl. Phys. A*, **222** (1974) 493.
[30] Guttormsen M., Ay K. O., Ozgur M., Algin E., Larsen A. C., Bello Garrote F. L., Berg H. C., Crespo Campo L., Dahl-Jacobsen T., Furmyr F. W., Gjestvang D., Görgen A., Hagen T. W., Ingeberg V. W., Kheswa B. V., Kullmann I. K. B., Klintefjord M., Markova M., Midtbø J. E., Modamio V., Paulsen W., Pedersen L. G., Renstrøm T., Sahin E., Siem S., Tveten G. M. and Wiedeking M., *Phys. Rev. C*, **106** (2022) 034314.
[31] Bokhovko M. V., Voevodskiy A., Kononov V., Poletaev E. and Timokhov V., Fiz.-Energ Institut, Obninsk Reports No. 2169 (1993).
[32] Shorin V., Kononov V. and Poletaev E., *Sov. J. Nucl. Phys.*, **20** (1975) 572.
[33] Wisshak K., Voss F., Arlandini C., Kaeppeler F. and Kazakov L., *Phys. Rev. C*, **61** (2000) 065801.
[34] Beer H., Walter G., Macklin R. and Pachet P., *Phys. Rev. C*, **30** (1984) 464.